Hydrothermal Synthesis of Nanoporous Metalofluorophosphates. 2. In Situ and ex Situ ^{19}F and ^{31}P NMR of Nano- and Mesostructured Titanium Phosphates Crystallogenesis

Christian Serre,[†] Chantal Lorentz,[‡] Francis Taulelle,*[,‡] and Gérard Férey[†]

Institut Lavoisier, UMR C8637, Université de Versailles-St-Quentin-en-Yvelines, 45 Avenue des Etats-Unis, 78035 Versailles Cedex, France, and RMN & Chimie du Solide, Tectonique Moléculaire du Solide, UMR 740, Université Louis Pasteur, 4 Rue Blaise Pascal, 67070 Strasbourg, France

Received November 5, 2002. Revised Manuscript Received February 3, 2003

The mechanisms of formation of the three-dimensional titanium phosphate πTiP and of H−TiP, a hexagonal mesotextured titanium(IV) fluorophosphate, were studied using in situ and ex situ ^{19}F and ^{31}P NMR experiments. In situ NMR indicated that the prenucleation building units (PNBU), forming the solids under hydrothermal conditions, are identical for both phases. A possible structure of the PNBU is provided. Ex situ ^{19}F and ^{31}P liquid NMR allowed the transformations occurring in the supernatant liquid to be followed. Two kinds of species were observed during both syntheses: reactive primary species, which are the less fluorinated titanium fluorophosphates, and passive primary species, that is, the highly fluorinated titanium fluorides and fluorophosphates, which act as a reservoir of reactive primary species by slow interconversion. πTiP crystallizes following a condensation, precipitation, dissolution, and re-crystallization process as shown by quantitative analysis of ex situ NMR of the solid state and X-ray powder diffraction. H−TiP is first mesotextured at room temperature, and then its inorganic walls redissolve and crystallize during hydrothermal aging.

Introduction

Synthesis of nanoporous materials follows usually a "trial and error" synthetic strategy or, at best, a combinatorial multidimensional parameter optimization. Rationalization of synthetic conditions is a demand to design properties of tailormade materials. Such a goal cannot be achieved without understanding the underlying rules of materials architecture and construction, the mechanism of formation, which is a key issue of materials design.[1−3]

Since the discovery of the M41S mesoporous silicate in 1992, a steady increase in the amount of research in this field has occurred. Several approaches of the mechanism of formation have been formulated, with emphasis on the initial stages of the synthesis.[4] Two different hypotheses have been considered,[4] a direct and a cooperative formation mechanism, but the last hypothesis is now generally accepted. The cooperative mechanism occurs in two steps. The first step is the formation of hybrid micelles, built up from surfactant micelles encapsulated by silicate species. These hybrid micelles interact to produce MCM-41 during aging.[5,6] Some propose that silicates layers form first, then cylindrical micelles intercalate the layers, and during aging the layers break and rearrange around the micelles to form MCM-41.[7,8]

Concerning nanoporous crystals, after a long and inconclusive period of attempts to rationalize zeolites syntheses via secondary building units, the mechanism of formation of an oxyfluorinated nanoporous aluminophosphate, $AlPO_4$−CJ2, has been determined by using in situ and ex situ NMR.[9] The dynamics of the different stages of the synthesis as well as the formation of the chemical bonds were obtained, leading for the first time to the characterization of a PNBU (prenucleation building units) during crystallization.[9,10] The method was further extended to aluminum polycations.[11] Since then, very recent results in zeolite chemistry appear to confirm the existence of PNBU and to succeed in avoiding most previous limitations.[12]

* To whom correspondence should be addressed. E-mail: taulelle@chimie.u-strasbg.fr.
[†] Université de Versailles-St-Quentin-en-Yvelines.
[‡] Université Louis Pasteur.

(1) Schüth, F. *Curr. Opin. Solid State Mater. Sci.* **2001**, *5*, 389.
(2) Cheetam, A. K.; Mellot, C. *Chem. Mater* **1997**, *9*, 2269.
(3) Walton, R.; O'Hare, D. *Chem. Commun.* **2000**, 2283.
(4) Beck, J. S.; Vartuli, J. C.; Roth, W. J.; Leonowicz, M.; Kresge, C.; Schmitt, K.; Chu, C. T.; Olson, D.; Sheppard, E.; Cullen, M.; Higgins, J.; Schenkler, J. L. *J. Am. Chem. Soc.* **1992**, *114*, 10834.
(5) Chen, C. Y.; Li, H. X.; Davis, M. E. *Microporous Mater.* **1993**, *2*, 17.
(6) Regev, O. *Langmuir* **1996**, *12*, 4940.
(7) Steel, A.; Carr., S. W.; Anderson, M. W. *J. Chem. Soc., Chem. Commun.* **1994**, 1571.
(8) Yanagisawa, T.; Shimizu, T.; Kuroda, K.; Kato, C. *Bull. Chem. Soc. Jpn*, **1990**, *63*, 680.
(9) Taulelle, F.; Haouas, M.; Gerardin, C.; Estournes, C.; Loiseau, T.; Férey, G. *Colloids Surf., A* **1999**, *158*, 299.
(10) Haouas, M.; Gerardin, C.; Taulelle, F.; Estournes, C.; Loiseau, T.; Férey, G. *J. Phys. Chim., Phys. Chim. Biol.* **1998**, *95*, 302.
(11) Allouche, L.; Gerardin, C.; Loiseau, T.; Férey, G.; Taulelle, F. *Angew. Chem., Int. Ed.* **2000**, *39*, 511.

10.1021/cm021347z CCC: $25.00
Published on Web 05/17/2003

Recently, several new, layered or three-dimensional, titanium phosphates and fluorophosphates crystals were reported in our group.[13] This study was extended to the synthesis of mesotextured hexagonal and lamellar titanium fluorophosphates with a semicrystalline framework.[14] During the study of the mesostructured solid, it appeared that applying thermal aging of this phase above 120 °C led to its transformation into πTiP, a pure inorganic three-dimensional solid with an open framework (see Supporting Information). Understanding this transformation, from a *meso*- to *nano*porous solid, was actually the starting point of this study. It was expected that a comparative in situ and ex situ NMR study of the formation of these two solids would shed some light on their formation mechanism and interconversion. The same methodology as the one used previously for $AlPO_4$−CJ2 was applied here to check if NMR signals of the PNBU can be observed.[15,16] After establishment of which titanium fluorides and fluorophosphate species exist in solutions by NMR,[17] an in situ and ex situ NMR study of the mechanism of formation of the two solids, the nanoporous πTiP and the mesoporous H−TiP, was undertaken and is presented here.

The structure determination of the PNBU was performed and the crystallization processes were studied. A mechanism of formation for both solids is eventually proposed.

Materials and Experiments

Sample Preparation. H−TiP, hexagonal mesostructured titanium(IV) fluorophosphates, was prepared according to previous studies using tetradecyltrimethylammonium bromide ($CH_3(CH_2)_{14}N(CH_3)_3Br$),[14] while tetramethylammonium hydroxide (TMAOH) was used for the inorganic three-dimensional titanium phosphate πTiP phase.[18,19] Molar ratios of TiF_4:H_3PO_4:organic agent:H_2O were 1:10:0.3:360 for both phases.

For both in situ and ex situ studies, samples were prepared according to the following procedure: 300 mg of TiF_4 (Aldrich 99%) was dissolved in 4.65 mL of deionized water and added to 1.65 mL of H_3PO_4 85% (Prolabo). Then, 200 mg of CTAB surfactant (Aldrich 99%) or 70 mg of TMAOH was dissolved in 8.7 mL of deionized water. The organic solution was slowly poured into the inorganic batch while stirring. During in situ experiments, the resulting suspension (phase H) or the clear solution (πTiP) was introduced into Teflon-lined NMR inserts as described in previous studies.[9,10] The temperature was progressively incereased to 100 °C (phase H) or 150 °C (πTiP). Once the final temperature was reached, NMR acquisition of ^{31}P or ^{19}F spectra started.

For ex situ experiments, hydrothermal syntheses were performed using Teflon-lined PARR bombs (23 mL) filled to 65% of their volume, heated at 100 °C (phase H) or 150 °C (πTiP) under autogenous pressure for different periods of time (0−45 h). Liquids and solids were separated. The solids were filtrated, washed with deionized water and acetone, and dried at 100 °C.

Elemental Analyses. Chemical elemental analysis for titanium, phosphorus, fluorine, carbon, nitrogen, and hydrogen contents was determined at the C.N.R.S. Central Laboratory of Analysis of Vernaison, France. Oxygen content was deduced by difference (%O = 100 − %(Ti + P + F + C + N + H)).

Physical Measurements. Thermogravimetric analyses were performed on a Texas Instrument TA 2050 analyzer under a nitrogen atmosphere at a 5 °C/min heating rate. X-ray powder diffraction patterns were acquired on a conventional high-resolution ($\theta-2\theta$) Bruker AXS Siemens D5000 diffractometer using $\lambda_{Cu\ K\alpha}$ in steps of 0.02° for 3 s/step with 1/01 mm slits. In situ NMR spectra were acquired on a MSL300 Bruker spectrometer with a 7.05 T magnetic field. ^{19}F spectra and ^{31}P were recorded at respectively 282.3611 and 121.4961 MHz. The pulse length of the simple pulse experiments was respectively 5 or 4.6 μs, with a 90° pulse of respectively 16.5 or 14 μs. A recycle delay of 10 s was used with 8 k of digitized points. The numbers of scans were respectively 48 (^{19}F) and 256 (^{31}P). Samples were introduced into special Teflon-lined NMR inserts.[9,10] Incremented acquisitions were separated by a period of 1 min.

Liquid- and solid-state ex situ NMR spectra were performed using respectively DPX 400 and DSX 500 Bruker spectrometers operating at respectively 9.39 or 11.7 T. ^{19}F resonates respectively at 376 and 470 MHz and ^{31}P at 161and 202 MHz. A VSP 10 mm probe was used for the liquid ex situ NMR experiments. A pulse length of 6.7 or 10 μs corresponding for both nuclei to the 90° pulse and recycle delays of 3 and 5 s with 32k or 8 k of digitized points respectively were used. The numbers of scans were 64 for ^{19}F and 128 for ^{31}P.

In both cases, liquid in situ or ex situ experiments, for ^{31}P, the spectral width was 65 ppm. For ^{19}F spectra, due to the very wide range of chemical shifts (>340 ppm), the spectra were recorded into two parts, one for the negative shifts (180 ppm) and a second for the positive shifts (200 ppm). Chemical shifts references were for ^{19}F, C_6F_6 $\delta = -163$ ppm relative to $CFCl_3$ at 0 ppm, and for ^{31}P, H_3PO_4 85% ($\delta = 0$ ppm).

Solid-state NMR spectra were acquired with a Bruker 4 mm MAS probe, with samples rotated at 20 kHz. ^{31}P spectra were recorded at 202 MHz with a pulse length of 1.5 μs and 2 s recycle delay and ^{19}F spectra were recorded at 470 MHz with a pulse length of 2.5 μs and a recycle delay of 2 s.

Results and Discussion

The purpose of this study is to study the formation of two solids, a mesostructured solid H−TiP and a crystalline titanium phosphate πTiP. The structure of πTiP or $Ti_2O(PO_4)_2{\cdot}2H_2O$ consists of a three-dimensional titanium phosphate built from dimers of titanium octahedra and phosphate groups (see Supporting Information). This delimits seven-membered rings channels along the *c* axis in which terminal water molecules point and interact through hydrogen bonds. The structure of the mesostructured titanium fluorophosphate H−TiP is unknown but a crystalline order appears upon hydrothermal aging, with a translation of 3.15 Å within the inorganic pore walls; this would correspond to a Ti−Ti or a Ti−P interactomic distance. πTiP and H−TiP are thermodynamically related since H−TiP turns into πTiP upon hydrothermal aging at a temperature above 120 °C.

Prenucleation Building Units

(1) In Situ Experiments. ^{19}F and ^{31}P in situ NMR experiments were performed for both phases. The temperatures were chosen respectively at 100 and 150 °C for the phases H−TiP and πTiP to obtain in situ experiments with a reasonable length (<1 day). As the solubility of titanium phosphates in water was very low (i.e., 10^{-3} M at pH = 1 at room temperature), we expected much lower signal intensities.

(12) Kirschhock, C. E. A.; Kremer, S. P. B.; Grobet, P. J.; Jacobs, P. A.; Martens, J. A. *J. Phys. Chem. B* **2002**, *106*, 4897.
(13) Serre, C.; Taulelle, F.; Férey, G. *Chem. Mater* **2002**, *14*, 998.
(14) Serre, C.; Hervieu, M.; Magnier, C.; Taulelle, F.; Férey, G. *Chem. Mater* **2002**, *14*, 180.
(15) Taulelle, F. *Curr. Opin. Solid State Mater. Sci.* **2001**, *5*, 397.
(16) Taulelle, F. *Solid State Sci.* **2001**, *3*, 795.
(17) Serre, C.; Corbiere, T.; Lorentz, C.; Taulelle, F.; Férey, G. *Chem. Mater.* **2002**, *14*, 4939.
(18) Bortun, A. I.; Khainakov, S. A.; Bortun, L. N.; Poojary, D. M.; Rodriguez, J.; Garcia, J. R.; Clearfield, A. *Chem. Mater* **1997**, *9*, 1805.
(19) Serre, C.; Guillou, N.; Férey, G. *J. Mater. Chem.* **1999**, *9*, 1185.

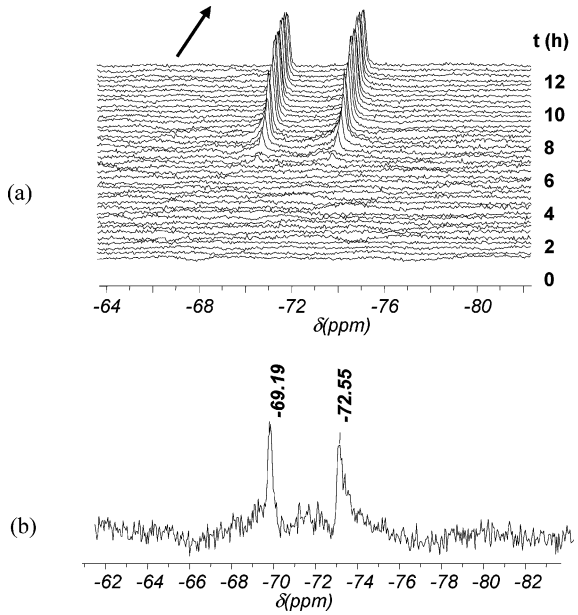

Figure 1. (a) In situ ^{19}F liquid NMR spectra as a function of time for πTiP at 150 °C. (b) Long acquisition in situ ^{19}F spectrum performed at the end of the in situ ^{19}F experiment of H−TiP at 100 °C.

(a) ^{19}F NMR. For πTiP, two signals at −68.8 and −71.2 ppm with a 1/1 ratio appear after 4−5 h (Figure 1a). Their intensity increases and reaches a plateau after 10 h. For H−TiP, two very weak signals are visible after 1−2 h and their intensities stabilize after 3−4 h (Figure 1b). A long in situ acquisition performed under the same temperature conditions at the end of the first experiment increases the signal-to-noise ratio of these two peaks and confirms definitely their presence. They exhibit a 1/1 ratio, at −69.2 and −72.5 ppm (insert of Figure 1b).

(b) ^{31}P NMR. For both H−TiP and πTiP, the intense signal of the free phosphates, due to the large excess of phosphoric acid used during the synthesis (P/Ti = 10), dominates at ≈0 ppm. After 3−4 h, two weak signals at −1.5 and −8.5 ppm with a 1/1 ratio appear (Figure 2a) with the peak at −1.5 ppm at the limit of detection. They increase to reach a maximum after 9−10 h.

For phase H−TiP, two very weak signals are visible after 2−3 h at −2 and −9.6 ppm. To confirm the presence of these weak signals, a long in situ acquisition is again performed at the end of the experiment. The signal at −9.6 ppm is clearly visible, and the signal at −2 ppm appears as a shoulder on the dominant signal (Figure 2b). Further experiments will confirm its existence (see ex situ results).

Despite low signal-to-noise ratios, especially for H−TiP, two signals, corresponding to a PNBU, are observed by ^{19}F and ^{31}P NMR. One must notice that almost identical chemical shifts are present in both cases. In addition, the PNBU exhibits the same characteristics as in $AlPO_4$−CJ2; it increases, then reaches a plateau, and is present at the end of the crystal formation. Actually, one can expect such behavior from classical nucleation theory. A first fast amorphous or gel phase appears, which redissolves in PNBU; after PNBU has reached supersaturation, nucleation starts, and the PNBU concentration plateaus in a stationary state during crystal growth.

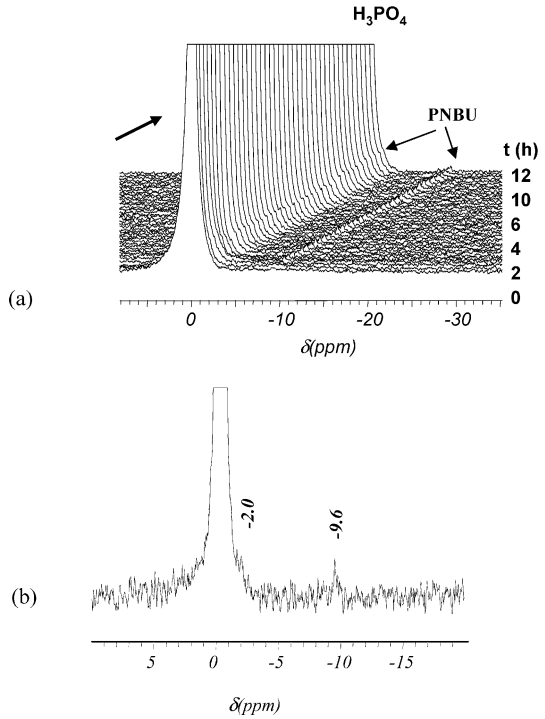

Figure 2. In situ ^{31}P liquid NMR spectra as a function of time for πTiP at 150 °C. (b) Long acquisition in situ ^{31}P spectrum performed at the end of the in situ ^{31}P experiment of H−TiP at 100 °C.

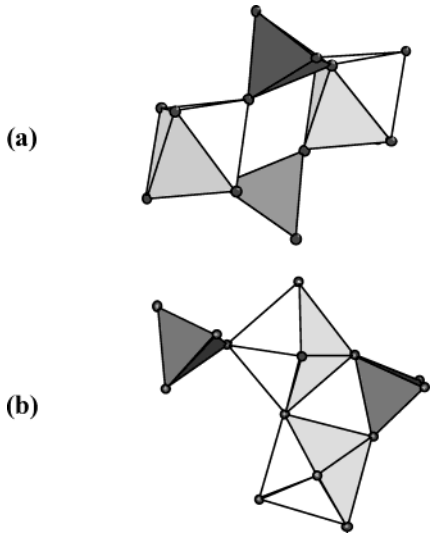

Figure 3. Proposed SBU (secondary building units) for phase πTiP: (a) Ti_2P_2 unit with Q2 phosphates; (b) Ti_2P_2 unit with Q1 and one Q2 phosphates.

Two factors can be taken into account for the intensity differences between the two syntheses. Compared with πTiP, the solubility of the PNBU for H−TiP is lower at a decreased temperature of 50 °C. As the nucleation surface is higher for the mesoporous compared to the nanoporous compound, the stationary state between the production of PNBU and its consumption decreases the supersaturation level.

Structure of the PNBU. Crystallizations of πTiP and H−TiP proceed therefore certainly through a common step involving the same PNBU. As no crystal structure of H−TiP exists, a determination of πTiP structure is needed to conjecture what could be the building units of the solids. As a reminder, in the case of $AlPO_4$−CJ2,

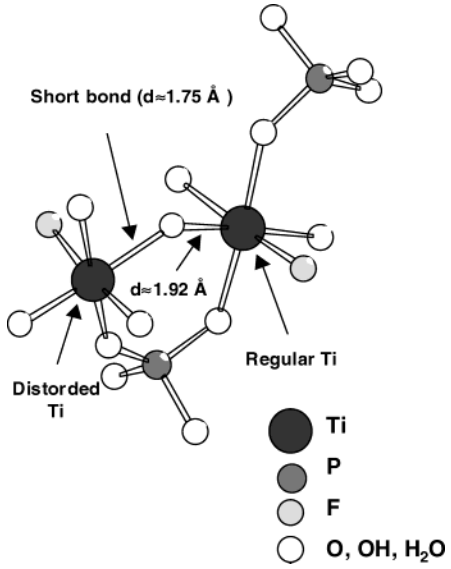

Figure 4. Proposed "ball-and-sticks" structure for the PNBU involved in the crystallization of H−TiP and πTiP.

it was demonstrated that the PNBU isomerizes in the SBU through a bridging bond formation of the 4R unit, indicating therefore that a strict identity between the PNBU and the SBU is not warranted.

For πTiP, two possible SBUs can be sketched from the crystallographic structure, both exhibiting a Ti_2P_2 stoichiometry (Figure 3). The first one consists of two crystallographically equivalent titanium octahedra connected only via two crystallographically equivalent phosphate groups with Q2 connectivity (full analogy with silicates terminology) (Figure 3a). The second possibility is a dimer of titanium octahedra with two inequivalent titanium atoms, connected to two inequivalent phosphate groups of Q2 and Q1 connectivities, one bridging the two titanium atoms and the other one connected to only one titanium atom (Figure 3b). At first sight, one might favor the simple 4-ring unit (4R) because, first of all, it seems to be a general condensation scheme for AlPO materials.[9,16,20] Second, this unique species may lead via a "clipping of the network into a crystal"[21] to two differentiated 4Rs in the final crystal. However, considering the chemical shifts observed during ^{31}P in situ NMR experiments ($\delta \approx -2$ and -9 ppm) and those deduced from ^{31}P liquid NMR experiments of the model solutions of titanium phosphates, a difference of 7 ppm would correspond to a change in metal−phosphorus connectivity. This excludes the 4R type of SBU. The PNBU is then a less symmetrical unit that contains two inequivalent phosphate groups with two different connectivities. A titanium dimer with two phosphate groups in asymmetric positions would do. A ^{19}F Cosy NMR experiment is performed to locate the fluorine atoms in the PNBU. Two possibilities exist. The two fluorines are either located on the same titanium atom or sit on two different titanium atoms. The experiment is run at room temperature using an ex situ supernatant liquid obtained after 15 h of synthesis of πTiP at 150 °C. No J_{F-F} coupling is observed (see Supporting Information), indicating that the two fluorines are not on the same titanium atom. Finally, previous studies on aluminophosphate indicated that the PNBU is an isomer of the two possible SBUs of πTiP (Figure 3a); in situ NMR indicated that the PNBU possess two phosphate groups of Q1 and Q2 connectivity (Figure 3b) while ex situ NMR showed that the two independent fluorine atoms are not grafted on the same titanium atoms. One can therefore conclude that the proposed structure of the PNBU consists of a dimer of titanium octahedra grafted with two phosphate groups of Q1 and Q2 connectivity and with one fluorine per titanium (Figure 4).

Table 1. ^{19}F NMR Chemical Shifts and Proposed Structures of Titanium Fluorides and Fluorophosphates According to Previous Studies (See References 17 and 22)[a]

chemical shift (ppm)	complexes	
−160	HF	obs.
76	TiF_6^{2-}	obs.
90(eq)/160(ax)	$TiF_5(H_2O)^-$	exch.
90(eq)/111(ax)	$TiF_5(H_2PO_4)^-$	obs.
120.5(eq)/192.4(ax)	$TiF_4(H_2O)_2$	exch.
112/125/181	$TiF_4(H_2PO_4)(H_2O)^-$	obs.
104/125	$TiF_4(H_2PO_4)_2^{2-}$	obs.
99.5/144	$TiF_3(H_2O)_3^+$	not obs.
119(eq)/139(ax)	$TiF_3(H_2PO_4)(H_2O)_2$	obs.
148/221.5	$TiF_3(H_2PO_4)_2(H_2O)^-$	not obs.
143	$TiF_3(H_2PO_4)_3^{2-}$	obs.
*	$TiF_2(H_2O)_4^{2+}$	not obs.
107/133	$TiF_2(H_2PO_4)(H_2O)_3^+$	obs.
*	$TiF_2(H_2PO_4)_2(H_2O)_2$	not obs.
135/152.5	$TiF_2(H_2PO_4)_3(H_2O)^-$	not obs.
*	$TiF_2(H_2PO_4)_4^{2-}$	not obs.
26	$TiOF(H_2O)_4^+$	obs.
*	$TiOF(H_2PO_4)_x(H_2O)_y$	not obs.
151(eq)/154(ax)	$Ti_xFa_yFb_{3y}(H_2PO_4)_zX_p$	obs.

[a] X = O, OH, F, H_2O, H_2PO_4. Abbreviations "eq" and "ax" refer to the equatorial and axial positions of the fluorine atoms within the titanium octahedra; "obs.", "not obs.", and "exch." are used in the last column respectively for species observed, not observed, and observed in exchange in our experimental conditions. The * refers to some theoretical complexes never observed up to now.

A comparison with the PNBU and SBU observed in the formation of $AlPO_4$−CJ2 is instructive. The PNBU of $AlPO_4$−CJ2 is a 4R unit. When included in the crystal, it isomerizes to form a 4R with a diagonal bridging bond between the two aluminum atoms of the initial 4R. In the case of πTiP, it looks like the same geometry imposes the opening of a Ti−O−P bond because of the significant tension of the ring containing a Ti−O−Ti bond. One may think therefore that the Ti−O−Ti bond is thermodynamically much stronger than the equivalent Al−OH−Al bond in CJ2. This is usually the case when comparing the strength of an oxo bond to that of a hydroxy bond. The Ti−O−Ti bond would therefore form first and will impede the 4-ring closure.

(2) Ex Situ Study. Ex situ analyses of liquids and solids were obtained from syntheses of phases πTiP and H−TiP stopped at times between 0 and 45 h. Each time, the supernatant and the solid were separated and analyzed by NMR, in liquid or solid conditions. Additionally, X-ray powder diffraction and quantitative analysis were made also on the solid fraction. The synthesis of πTiP was conducted at 150 °C while the phase H−TiP was synthesized in two steps, a period of stirring at room temperature followed by aging at 100 °C.

(20) Rao, C. N. R.; Natarajan, S.; Choudhury, A.; Neeraj, S.; Ayi, A. A. *Acc. Chem. Res.* **2001**, *34*, 80.
(21) Allouche, L.; Huguenard, C.; Taulelle, F. *J. Phys. Chem.* **2001**, *62*, 1525.

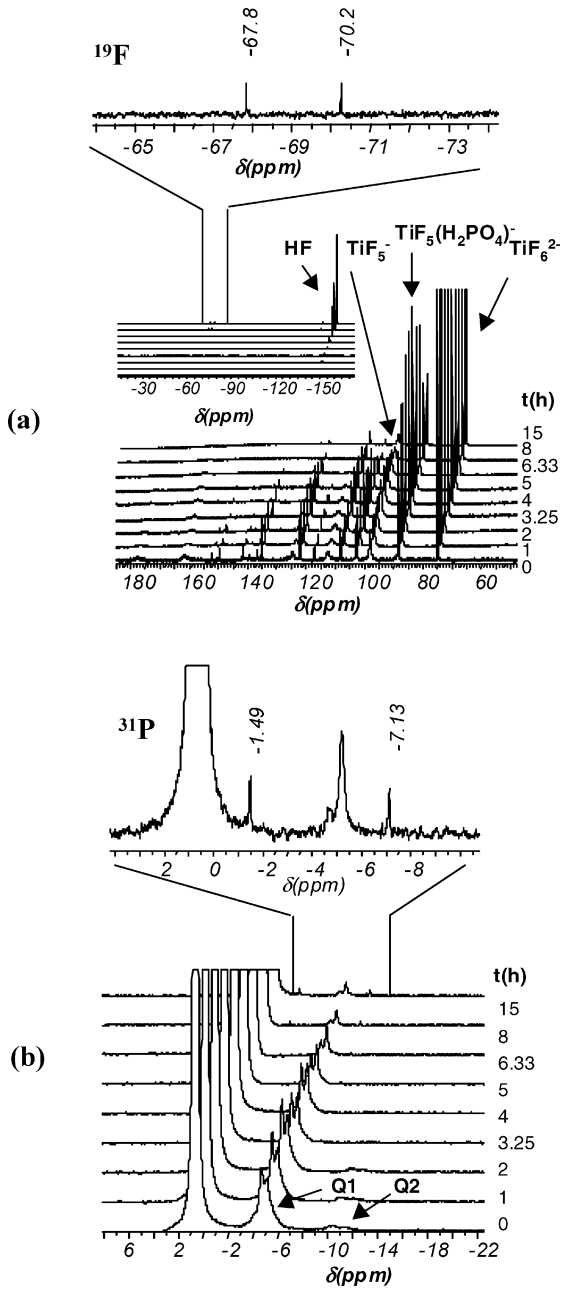

Figure 5. Ex situ liquid NMR spectra as a function of time for πTiP: (a) ^{19}F; (b) ^{31}P. The inserts at the left of each figure represent the negative chemical shifts part of the spectra; enlargements of the spectra obtained after 15 h and showing the signals of the PNBU are included at the top of each figure.

In our conditions, HF, titanium fluorides, and titanium fluorophosphates monomeric species are present in solution. Following previous studies of model solutions,[17,22] the monomeric species are known (Table 1) and only small amounts of oligomeric complexes are observed.

(a) Ex Situ NMR Analyses of the Liquid Fraction. (i) Phase πTiP. ^{19}F NMR. The evolution of the different species in solution is displayed in Figure 5a. A global decrease of the fluorophosphate complexes and an increase in HF occur during the synthesis. Some species, such as $TiF_5(H_2PO_4)^{2-}$, exhibit singular behavior, increasing first and then decreasing at the end of the synthesis. Interestingly, the PNBU signals appear at −67.8 and −70.2 ppm after 5 h and their intensity increases with time. The evolution of integrated NMR signals is displayed in Figure 6.

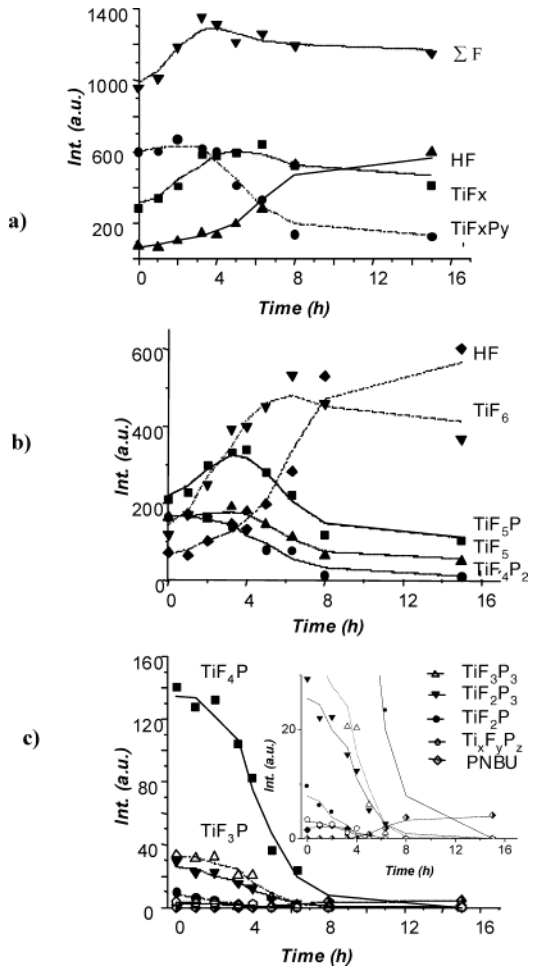

Figure 6. Evolution of the relative concentration of the fluorinated complexes present in the liquid phase as a function of time during the synthesis of πTiP at 150 °C: (a) different types of species; (b) the passive primary species; (c) the reactive primary species. In the latter case, an enlargement is included at the top right of the figure. For a better understanding, only the approached formulas of the complexes are given.

The total amount of fluorine in solution increases with time. This is well correlated with precipitation of πTiP, which does not contain any fluoride, and releases them in solution (Figure 6a). Titanium fluorophosphate complexes disappear during the first 8 h of the synthesis, generating HF in solution and leading to an increase in titanium fluorine concentration. After 8 h, fluorophosphates are no longer consumed and the concentration of titanium fluorides decreases slightly with time.

Two kinds of primary species can be distinguished from these results: "Passive primary species" are the titanium fluorides and the highly fluorinated titanium fluorophosphates ($TiF_5(H_2PO_4)^{2-}$, $TiF_4(H_2PO_4)_2^{2-}$) whose concentrations increase or remain stable during the first hours of the synthesis and decrease partially at the end of the synthesis (Figure 6b). "Reactive primary species " correspond to the less fluorinated complexes ($TiF_3(H_2PO_4)_3^{2-}$, $TiF_2(H_2PO_4)_3^{-}$, etc.). They are completely consumed during the first 8 h of the synthesis

(22) Chernyshov, B. N.; Davidovich, R. L.; Didenko, N. A.; Logvinova, V. B.; Buslaev, A. *Coord. Chem.* **1986**, *12*, 1638 (in Russian).

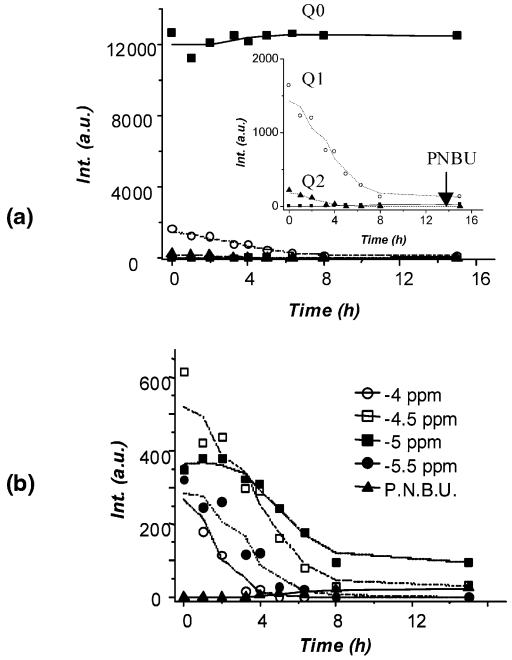

Figure 7. Evolution of the relative concentration of the phosphated complexes present in the liquid phase as a function of time during the synthesis of πTiP at 150 °C: (a) different types of species (Q0, Q1, and Q2); an enlargement of the Q2 species is represented as an insert at the right of the figure. (b) The four types of Q1 complexes.

(Figure 6c). Finally, the PNBU intensity increases between 5 and 10 h to reach a plateau toward the end of the synthesis.

^{31}P NMR. The same type of evolution observed previously with ex situ ^{19}F liquid NMR is observed using ^{31}P NMR, even if the resolution is worse than those obtained with ^{19}F NMR (Figure 5b). Complexes progressively disappear during the synthesis and signals of PNBU appear after 5 h at −1.5 and −7.15 ppm with their intensity increasing with time. In Figure 7, ^{31}P results are plotted. Q1 complexes are partially transformed during the first 8 h while Q2 species are totally consumed after 3−4 h (Figure 7a). Four Q1 peaks are observed, exhibiting different behavior (Figure 7b): "reactive primary species" ($\delta = -4$ and -5.5 ppm) and "passive primary species" ($\delta = -4.5$ and -5 ppm). These latter complexes correspond to the highly fluorinated $TiF_5(H_2PO_4)^{2-}$ and $TiF_4(H_2PO_4)_2^{2-}$ species. The characteristic time of the synthesis is close to 8 h, which is in agreement with ^{19}F results, and the PNBU intensity signal increases with time after 4 h.

(ii) Phase H−TiP. ^{19}F NMR. The evolution of the different species in solution is displayed in Figure 8. A global decrease in the concentration of the complexes (the passive primary species) occurs, however, less pronounced compared with πTiP, while the amount of HF increases. The same singular behavior is seen for species such as TiF_6^{2-} as for the πTiP phase, decreasing first and then increasing at the end of the synthesis. The PNBU signals appear at −69 and −71.5 ppm during the aging period, and their intensity increases with time.

Figure 9a shows that the concentration of the fluorinated species decreases during the first moments of the synthesis at room temperature; then, during aging, titanium fluorophosphates are slowly consumed while

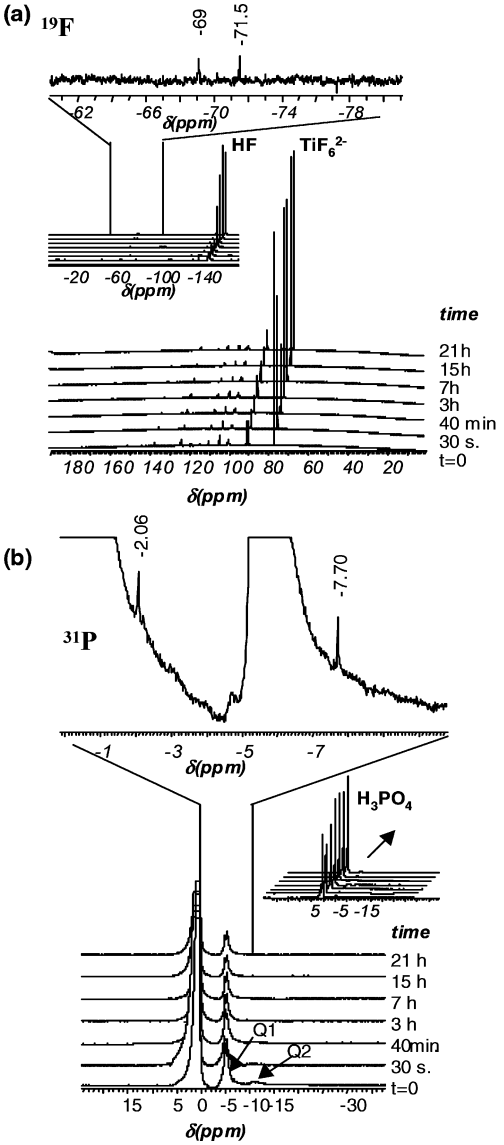

Figure 8. Ex situ ^{19}F (a) and ^{31}P (b) liquid NMR spectra of phase H. As a function of time, without the structuring agent at $t = 0$, with structuring agent at room temperature at $t =$ 30 s and $t = 40$ min, and at 100 °C as a function of time ($t \geq$ 3 h). The insert at the top of a) represents a global view for the negative chemical shifts part of the spectra and the insert at the top of b) represents the enlargement of the last spectrum showing the signals of the PNBU.

titanium fluorides and HF are released. These results indicate that a highly fluorinated solid precipitates during the first step of the synthesis while the solid releases fluorine during aging. After 10−15 h, no evolution is observed in the liquid phase.

Two types of complexes are again present: the passive primary species and the reactive primary species (Figure 9b,c). However, the situation is more complex than with πTiP. At room temperature, all "reactive" or "passive" primary species are more or less consumed. During the hydrothermal aging, only the reactive primary species, that is, the less fluorinated complexes ($TiF_3(H_2PO_4)_3^{2-}$, $TiF_2(H_2PO_4)_3^{-}$, and the oligomeric complex $Ti_xF_y(H_2PO_4)_zX_n$), keep on being consumed during the first hours of aging (Figure 9b,c) while the concentration of the passive primary species (HF, titanium fluorides, and other titanium fluorophosphates) remains approximately stable.

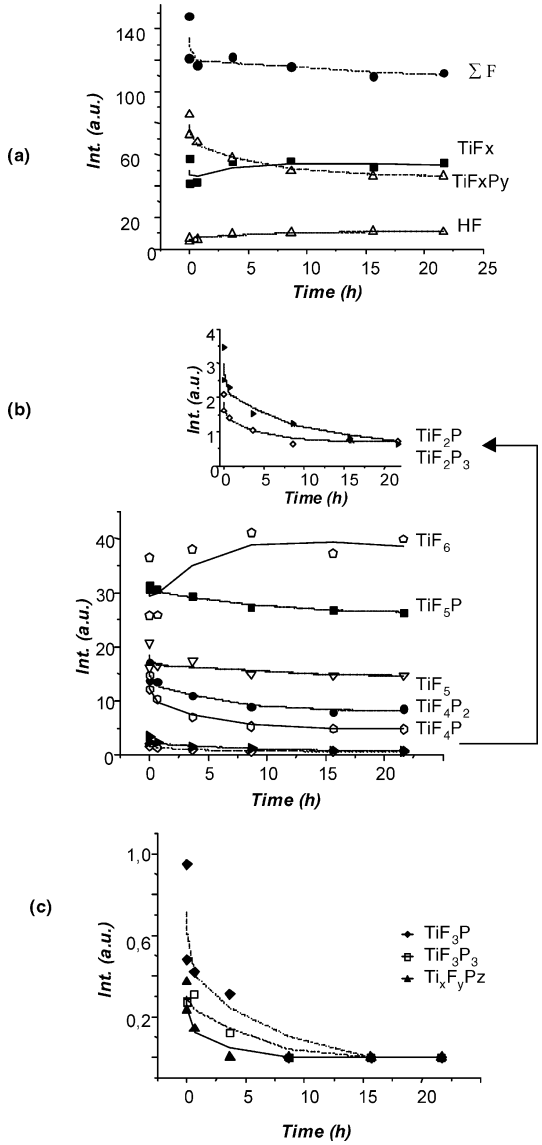

Figure 9. Evolution of the relative concentration of the fluorinated complexes present in the liquid phase as a function of time during the synthesis of phase H at room temperature (t = 30 s, 40 min) and at 100 °C ($t \geq 3$ h): (a) different types of species; (b) the passive primary species; (c) the reactive primary species. In the latter case, an enlargement is included at the top right of the figure. For a better understanding, only the approached formulas of the complexes are given.

^{31}P NMR. In Figure 8b, one can see that the passive primary species disappear progressively during the synthesis and that PNBU signals appear during the aging treatment at −2.06 and −7.7 ppm with their intensity increasing with time. This result confirms the existence of these ^{31}P PNBU signals observed, with a very low signal-to-noise ratio, during in situ ^{31}P NMR experiments. ^{31}P experiments show that Q1 complexes are essentially consumed during the first 3−4 h and their concentration is stable after 15 h (Figure 10a, b). Q2 phosphate complexes are totally consumed after 3 h (Figure 10a). No significant difference in behavior is observed for the individual Q1 species (Figure 10b).

(b) Ex Situ NMR Analyses of the Solid Fraction. (i) Phase πTiP. No solid appears before 2 h. After 2 h, a colloidal suspension is obtained. After 3 h, a white precipitate appears. Both XRD and ^{31}P solid-state NMR

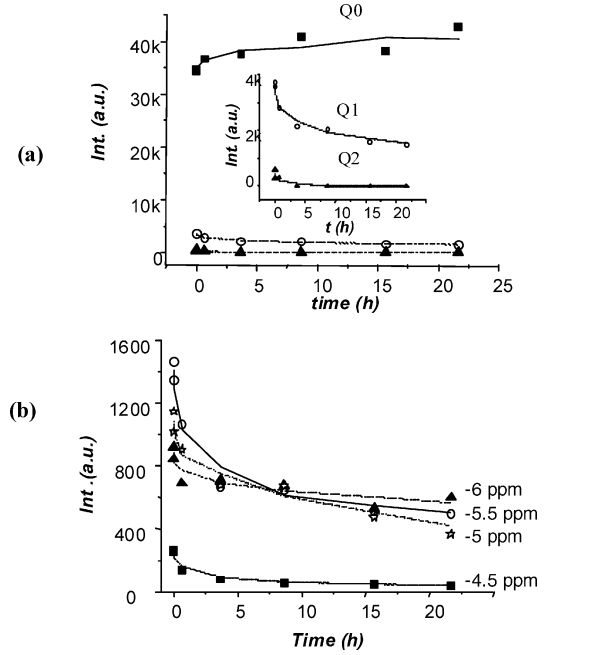

Figure 10. Evolution of the relative concentration of the phosphated complexes present in the liquid phase as a function of time during the synthesis of phase H at room temperature (t = 30 s, 40 min) and at 100 °C ($t \geq 3$ h): (a) different types of species (Q0, Q1, and Q2). (b): the four types of Q1 complexes.

indicate that an unknown intermediate phase, denoted TiOP, crystallizes between 2 and 4 h (Figure 11). After 4 h, TiOP is consumed while the crystal growth of πTiP begins.

TiOP refers to a layered titanium phosphate reported recently by Clearfield et al.[23] Its structure is still unknown but the authors clearly demonstrated that this solid exhibits a two-dimensional structure and a Ti_2O_3-$(H_2PO_4)_2 \cdot 2H_2O$ stoichiometry. In our case, the crystallinity was however not good enough to determine its crystal structure.

The yield of the reaction was measured (see Supporting Information). It shows that the reaction reaches a 67% yield in titanium after 15 h. Quantitative analysis indicates that the P/Ti stoichiometry during the synthesis remains constant while O/Ti (calculated) decreases from 6.5 to 5.5 between 4 and 8 h of synthesis (see Supporting Information). This is consistent with a phase transformation of phase TiOP into πTiP.

(ii) Phase H−TiP. XRD shows that H−TiP is textured at the very first moments of the synthesis at room temperature (Figure 12). Upon aging, the structure remains and an extension of the hexagonal domains occurs since intensities of the 110, 200, and 210 peaks increase. As described before, the inorganic pore walls crystallize after a few hours of aging, as indicated by the presence of the 3.15 Å high-angle reflection. ^{19}F and ^{31}P solid-state NMR (insert of Figure 12) indicate that inorganic walls of H−TiP formed at room temperature are not crystalline and it is only during hydrothermal aging that crystallization of the walls takes place.

At room temperature, ^{19}F peaks at 80−100 ppm are observed after 30 s and their intensities decrease with

(23) Bortun, A. I.; Bortun, L.; Clearfield, A. *J. Mater. Res.* **1997**, *11*, 2490.

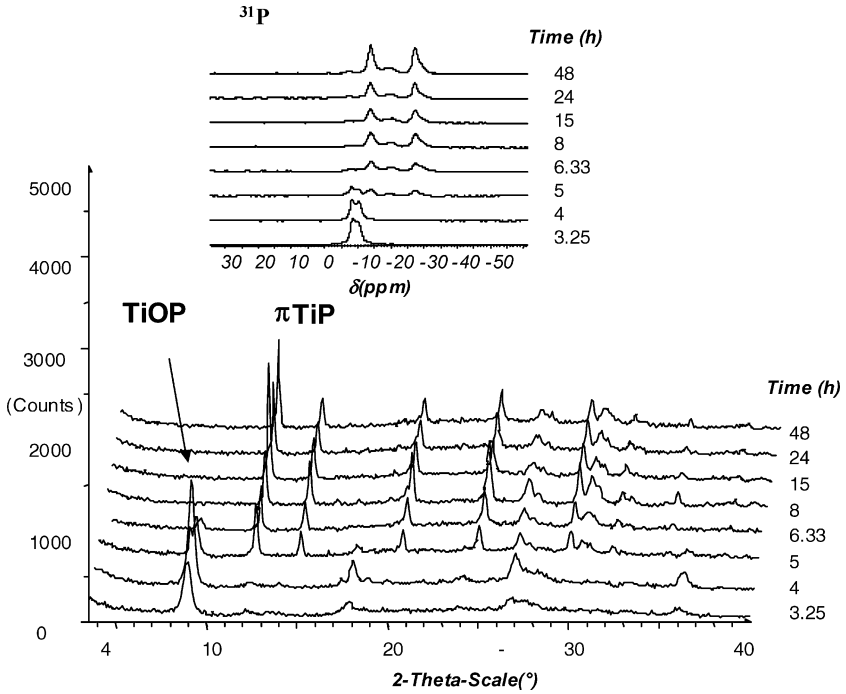

Figure 11. XRD pattern of ex situ solids of the synthesis of πTiP as a function of time. The ^{31}P solid-state NMR spectra of the corresponding solids are represented as an insert at the top of the figure.

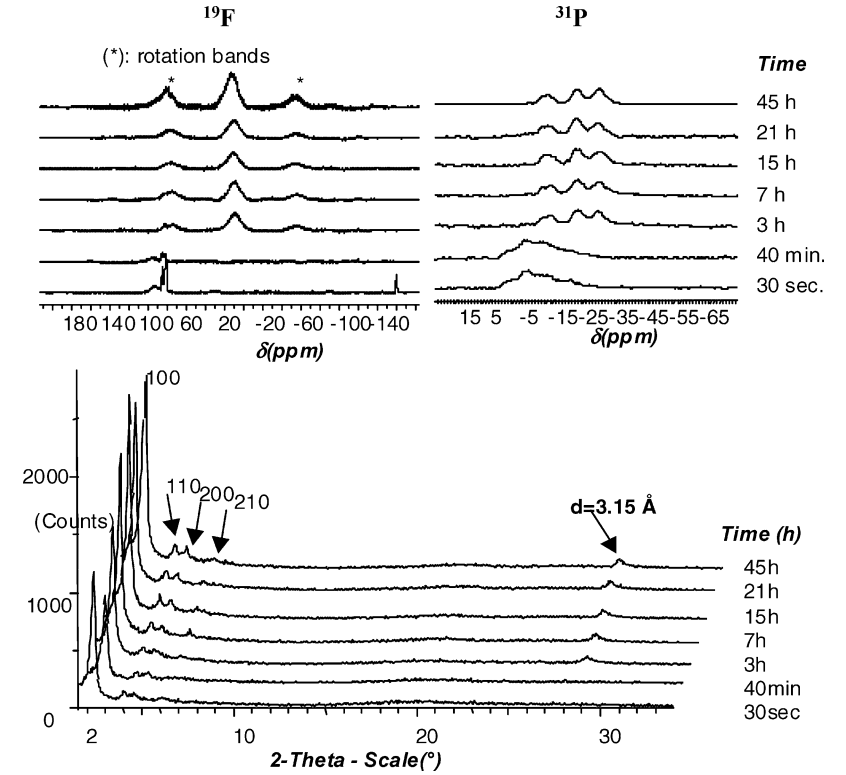

Figure 12. XRD pattern of ex situ solids of the synthesis of H−TiP as a function of time. The ^{31}P and ^{19}F solid-state NMR spectra of the corresponding solids are represented at the top of the figure.

time. According to the chemical shifts observed during liquid ^{19}F NMR experiments, these values correspond to highly fluorinated titanium fluorides or fluorophosphates. ^{31}P NMR shows only a broad distribution of signals at values between 0 and −20 ppm. During aging, the former ^{19}F peaks have disappeared and one broad ^{19}F peak is present at +10 ppm and the broad ^{31}P distribution is replaced by three peaks at −12, −26, and −30 ppm. As discussed before, these signals would correspond respectively to terminal Ti−F bond and to Q2, Q3, and Q4 metal−phosphorus connectivity.

The yield of the synthesis has been measured (Figure 13). At room temperature, a relatively small amount of solid is formed (yield ∼ 20%). Quantitative analysis indicates that the initial precipitate is rich in fluorine and surfactant, in agreement with the ^{19}F solid-state NMR results. Hydrothermal aging leads to a doubling of the titanium yield after 10 h and, at the same time,

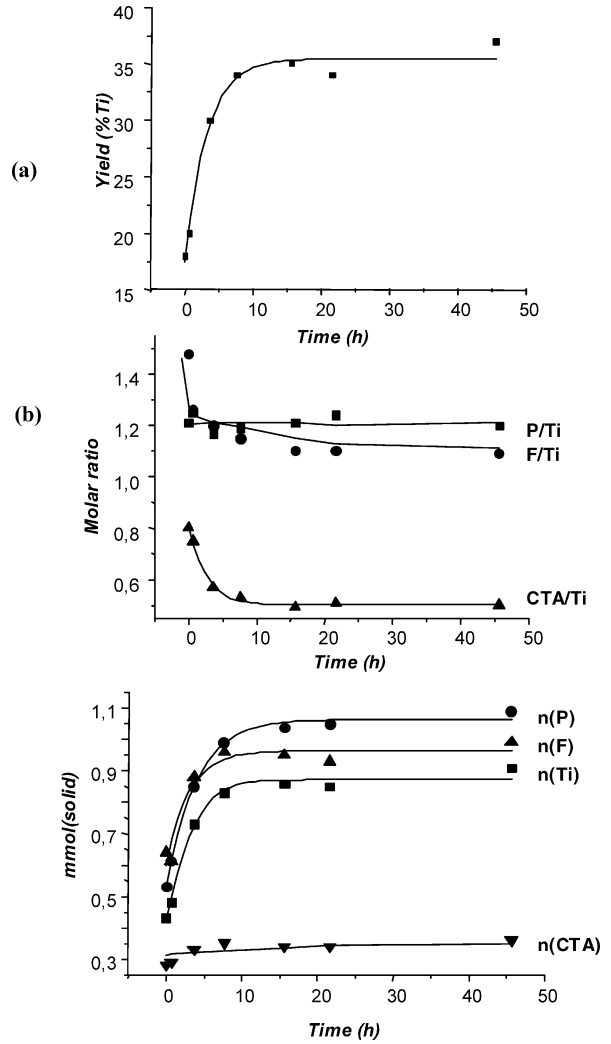

Figure 13. (a) Yield in titanium of the synthesis of H−TiP as a function of time. (b) P/Ti, F/Ti, and CTA/Ti ratios deduced from quantitative analysis, as a function of time. (c) Number of moles of each component (Ti, F, P, CTA) as a function of synthesis time.

to a decrease of surfactant and fluorine ratios. The resulting composition of the solid is P/Ti = F/Ti = 1 and CTA/Ti = 0.5. The proportion of surfactant remains almost stable upon aging while a strong increase in titanium, phosphorus, and fluorine, with P/Ti and F/Ti ratios close to 1, occurs while aging. This stoichiometry corresponds to the PNBU proposed previously.

(c) Mechanisms of Formation. (i) Phase πTiP. On the basis of in situ NMR and ex situ results, a tentative formation mechanism of πTiP at 150 °C is proposed. During the first 2 h of the synthesis, no solid is formed and a condensation process is engaged. The reactive primary species, that is, the less fluorinated titanium fluorophosphates, are slowly consumed. HF is released and the concentration of the passive primary species, that is, the titanium fluorides and the highly fluorinated $TiF_5(H_2PO_4)^{2-}$ and $TiF_4(H_2PO_4)_2^{2-}$ complexes, increases. Between 2 and 4 h, this condensation process accelerates and a layered titanium phosphate (TiOP) precipitates. Between 4 and 8 h, πTiP crystallizes at the expense of the intermediate TiOP. The reactive primary species is totally consumed while HF is still released and the passive primary species eventually disappears. The PNBU appears and its concentration increases with time. After 8 h, TiOP is consumed. The crystal growth of πTiP goes on and the concentration of the PNBU still increases.

(ii) Phase H−TiP. A similar approach is proposed for the hexagonal phase sketched. This phase is built up in two steps: one at room temperature and one during aging (100 °C). During the first stage, a hexagonal mesophase with amorphous inorganic walls and highly fluorinated surfactant salts forms immediately. In the liquid phase, the formation of the surfactant salts leads to an unexpected partial consumption of passive primary species, that is, the titanium fluorides and the highly fluorinated titanium fluorophosphates. The partial decrease in the concentration of the reactive primary species, that is, the less fluorinated fluorophosphates $TiF_3(H_2PO_4)_3^{2-}$, $TiF_2(H_2PO_4)_3^{-}$, and the oligomeric complex $Ti_xF_y(H_2PO_4)_zX_n$) is due to the precipitation of the phase H−TiP. During the first hours of aging, the walls of the mesophase crystallize and the size of the hexagonal domains increases. The crystallization of the walls originates most probably from the PNBU, accompanied by a significant liquid-to-solid mass transfer. In liquid phase, the reactive primary species are partially consumed while the concentration of the PNBU increases with time. Surfactant salts are dissolved together with a release of HF and a generation of the passive primary species. After 10−15 h of aging, the reaction is finished.

(d) Comparative Approach. A global comparative approach of the formation of the two titanium phosphates is finally given (Figure 14). Starting from an aqueous source of titanium complexes, fluorides, and fluorophosphates, of monomeric or oligomeric structure, the presence of either small organic cations (TMA^+) or cationic micelles (CTAB) leads to respectively πTiP or H−TiP phases. At first sight no direct relationship exists between the two solids: a three-dimensional hydrated titanium phosphate (πTiP) and a mesotextured hexagonal titanium fluorophosphate (H−TiP). The formation of the inorganic πTiP phase is based on a condensation, precipitation, and dissolution−recrystallization process with the presence of an intermediate compound, the hydrated two-dimensional titanium phosphate (TiOP). H−TiP is formed in two steps: first, at room temperature, a mesotextured solid with amorphous inorganic walls precipitates together with highly fluorinated surfactant salts. Hydrothermal aging (100 °C) leads to crystallization of the walls and dissolution of the salts. Aging at a temperature above 120 °C leads, however, to the dissolution of the mesotextured solid to produce TiOP and eventually πTiP.

In both cases, the PNBU, of proposed formula $Ti_2OF_2(HPO_4)(H_2PO_4)X_5$ (X = OH, H_2O), participates in the crystallization of solids under hydrothermal conditions.

Conclusions

Despite the initial difficulties of the chosen system, low solubility, and no NMR observability of titanium, the comparative study of the formation of two apparently nonrelated solids, πTiP and H−TiP, respectively, nano- and mesostructured phases, allowed us to propose a candidate for the PNBU involved in both crystallization processes. Surprisingly, it appears that the PNBU is the same in both cases, confirming the thermody-

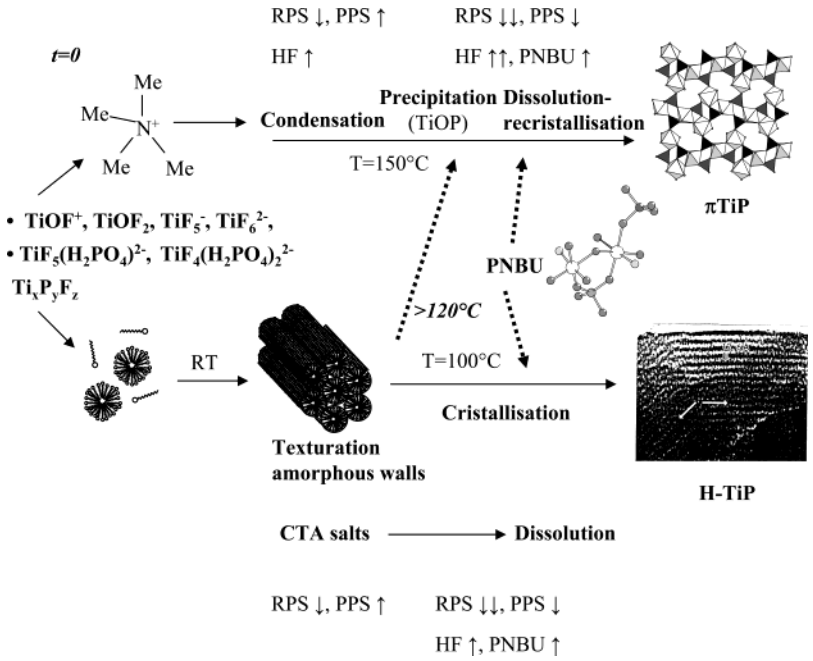

Figure 14. Schematic and comparative global approach of the formation mechanism of πTiP and H−TiP. RPS = reactive primary species; PPS = passive primary species.

namical relationship between the phases considered, observed previously. A structural model for the PNBU has been established and consists of a dimer of titanium octahedra grafted by two phosphate groups, one bridging the two titaniums and the other terminal, and two fluorine atoms.

The ex situ study confirmed the existence of the PNBU and provided information about the evolution of the concentration of the fluorinated and phosphated complexes upon the synthesis time for both solids. Global and qualitative trends concerning their formation mechanisms could be proposed. Finally, these results show that the "in situ and ex situ" methodology introduced previously can be furthered to the formation of mesoporous as well as nanoporous compounds. Though up to now no direct technique can evidence low concentration of species (supersaturated) that become included in the crystalline phase, the combination of in situ and ex situ NMR and XRD allows limitation of the possibilities and proposal of good PNBU candidates.

In situ and ex situ ^{19}F and ^{31}P NMR are used to investigate the mechanisms of formation of a 3D πTiP and of a hexagonal titanium fluorophosphate In situ results indicate a common prenucleation building unit (PNBU) for both solids under hydrothermal conditions. Two types of primary species are evidenced, passive and reactive toward the PNBU. The passive species are the most fluorinated. The tentative structure of the PNBU is provided. The formation of the two phases involves precipitation−redissolution−crystallization under hydrothermal conditions.

Acknowledgment. The CNRS, the French Ministry of Research, and RHODIA are gratefully acknowledged for their financial support.

Supporting Information Available: Additional supporting figures (PDF). This material is available free of charge via the Internet at http://pubs.acs.org.

CM021347Z